Inertial Electrostatic Confinement Fusion Device Source of X-Ray Radiation

Gamal M. Elaragi[1*]

[1] Plasma Physics and Nuclear Fusion Department, Nuclear Research Center, EAEA, Cairo, Egypt

Email Address

elaragi@gmail.com (Gamal M. Elaragi)
*Correspondence: elaragi@gmail.com

Received: 14 December 2017**; Accepted:** 28 December 2017

Abstract:

The aim of this paper introduces the preliminary results of the design and construction of first Egyptian inertial electrostatic confinement IEC fusion device. It consists of 2.8 cm stainless steel cathode, 6.5 cm anode diameter with 10 cm diameter 30 cm height vacuum chamber. The operation of IEC experiments has concentrated on pulsed operation to achieve the high currents required to generate increased reactions rates. The discharge voltage waveform with peak voltage 20kV and current pulse waveform has been registered using pick-up coil with peak current about 170mA. Experiments are performed with nitrogen as operating gas at different pressures and voltages. Time resolved of x-ray radiation signals are obtained using fast radiation detector.

Keywords:

Detector, Plasma, Vacuum, Waveform, X-Rays

1. Introduction

In IEC devices, fusion ions are electrostatically accelerated through a spherically symmetric central focus point. At the focus point they are at sufficiently high energy to overcome their mutual electrostatic repulsion that some small fraction of the ions will fuse and release energy in the form of high energy fusion products [1]. The IEC fusion device basically consists of a spherical-gridded cathode concentrically placed at the center of a spherical anode filled with a fuel gas. A glow discharge takes place between these electrodes. The produced ions are then accelerated toward the center through the transparent gridded cathode undergoing fusion reactions. Fusion reactions in spherical inertial electrostatic confinement (SIEC) devices were first realized by Hirsh [2, 3] using high energy ion guns as a source of ions. Miley et al. [4, 5] carried out experiments using a transparent grid as cathode and a spherical glow discharge as ion source. In their experiments, although the measured neutron production rate was a fraction [6] of that of Hirsh's data, the dependence of the neutron production rate on the device parameters was similar to that of Hirsh.

For instance, an IEC neutron generator [7] of 20 cm in diameter demonstrated more than 6 kW discharge power to produce 10E7 neutrons/sec for D-D fusion. Both the input power and the neutron output are high in contrast with a typical commercial sealed neutron tube [8] with similar size, which generates

~10E6 neutrons/sec for D-D (~10E8 n/sec for D-T) with ≈ 9 W. The improvement of charged particle confinement in IEC systems is of paramount interest for higher intensity neutron sources and possible IEC fusion power plants. Sedwick and McGuire proposed a method of improving ion confinement times by electrostatically focusing ion beams to keep them away from cathode grid wires [9]. A Neutron/Gamma-ray combined inspection system for hidden special nuclear materials (SNMs) in cargo containers has been developed in Japan. The inertial electrostatic confinement fusion device has been adopted as neutron source have been developed to realize the fast screening system. The prototype system has been constructed and tested in the Reactor Research Institute, Kyoto university [14]. Inertial Electrostatic Confinement (IEC) plasma systems were investigated experimentally at the University of Kentucky with air and argon as working gas at pressure levels between 10 and 100 mTorr and at electrical powers up to 60 W clearly aiming at non fusion IEC operation. Initial emission spectroscopy measurements were carried out confirming the presence of heavy particles in the IEC beam. From the interaction of the IEC beam with an aluminum foil target in combination with the emission spectroscopy results, first estimates of heavy particle velocities and potential thrust of this system were obtained to be in the range of 5-6.4 km/s and about 1 mN, respectively [15].

2. Experimental Set-Up

The IEC consists of a cylindrical vacuum chamber made of Pyrex glass tube with 10 cm of diameter and 30 cm height. The inner electrode consist of two stainless steel rings which are welded in their joint places (Fig. 1) and spiral outer electrode made of stainless steel. Figure 1 displays schematic diagram of the construction details of the IEC fusion set-up. Table 1 shows some parameters of IEC fusion device. The vacuum system consists of a rotary pump (Edwards single stage model 1 Sc.-150B). To avoid vapor from back streaming, the vacuum chamber is washed by gas after evacuation by the rotary pump.

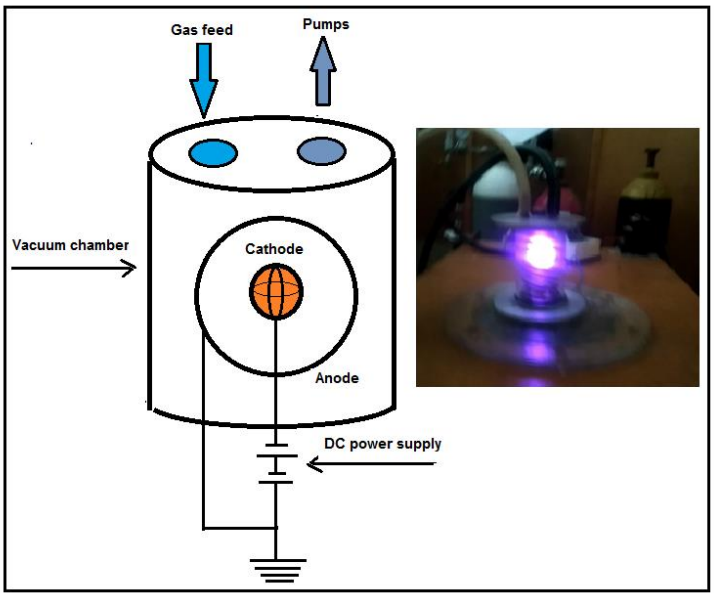

Figure 1. *Schematic diagram and photo of experimental setup.*

The gas was fed into the system via a flow meter in OMEGA model. The pressure was measured using a thermocouple gauge in Edwards's model.

Table 1. *Design and operational parameters of IEC fusion device.*

Parameter	Value
Vacuum chamber diameter	10 cm
Vacuum chamber height	30 cm
Anode grid diameter	6.5 cm
Cathode grid diameter	2.8 cm
High-voltage Stalk height	12 cm
Cathode voltage	25 kV
Gas pressure	0.001-1 Torr

2.1. High Voltage System

A power supply, transformer 20kV and high voltage diodes have been used for this purpose. During the first positive half-cycle, which is designated on the sine wave graph as T1, the voltage from the transformer increases accordingly with the polarity shown. The current flows in the direction of the arrows, charging the capacitor through the diode. During the capacitor charging time there is no voltage to the inner grid because the current takes the course of least resistance. In other words, rather than take a path through ground and up to the plate of the cathode, the current swings up through the diode. The voltage across the capacitor will rise to the transformer secondary voltage to the maximum 20kV volts. As the transformer secondary voltage begins to decrease from its maximum positive value (at time increment T2 on the sine wave graph), the capacitor will attempt to discharge back through the diode. The diode is like a one-way street in that it will not conduct in this direction. Thus, the discharge path is blocked, and the capacitor remains charged to the 20kV volts.

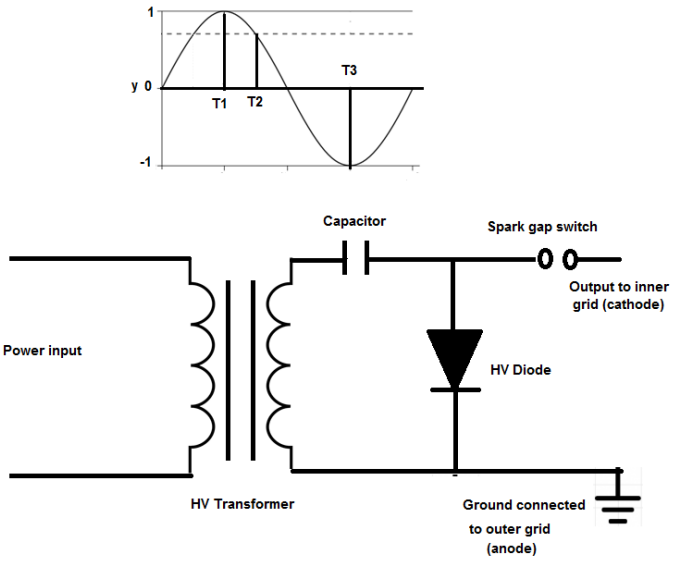

Figure 2. *Circuit diagram of the power supply.*

At time T3, the transformer secondary (output) voltage swings into the negative half-cycle and increases in a negative direction to a negative 20kV volt. The transformer secondary and the charged capacitor are now essentially two energy sources in series. The 20kV volts across the transformer winding add to the 20kV volts stored in the capacitor and the sum voltage of 40kV volts is applied to the cathode. There are two fundamental characteristics of this 40kV-volt output that

should be noted. First, because a voltage double is also a rectifier, the output is a DC voltage. Second, the resulting output voltage that is applied to the cathode is actually a pulsed DC voltage. This is because the double generates an output only during the negative half-cycle of the transformer's output (secondary) voltage. So, the inner grid is, in fact, pulsed on and off at a rate of 50 times per second. Thus the voltage double circuit has been used to conduct the spark gap (S.G.).

3. Results and Discussion

The applied voltage to and the discharge current through the discharge chamber were measured using a voltage divider (homemade), which was connected between the two electrodes, and a current monitor, which can be located upon returning to the ground. The signals from the voltage divider and the current monitor were recorded in a digitizing oscilloscope (Lecroy, USA) with 200 MHz bandwidth. Figures 3 and 4 indicate the current and voltage waveforms characterizing the pulsed IEC fusion device.

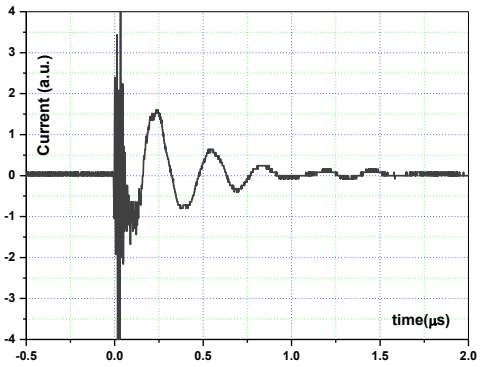

Figure 3. *Discharge current signal from IEC plasma.*

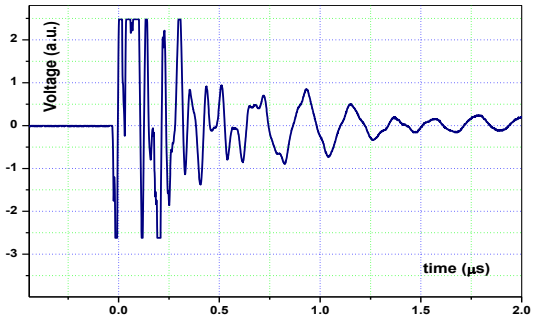

Figure 4. *Discharge voltage signal from IEC plasma.*

The light emitted by the plasma in the observation region was collected with an optical fiber and guided to a photomultiplier. A Hamamatsu photomultiplier tube (PMT) was used to detect coincident optical response. This PMT was mounted above and offset to the side of the plasma source, at a distance of 5 cm from the plasma source and the output signal was measured and recorded directly by a digitizing oscilloscope (Lecroy, USA) with a 200-MHz bandwidth (figure 5).

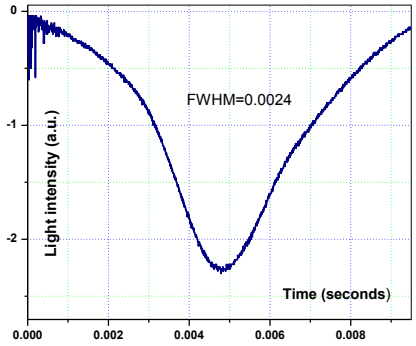

Figure 5. *PMT signal of IEC plasma Source.*

Typical photomultiplier signals correspond to plasma structures in the reactor for different gases can be observed. The photomultiplier voltage traces includes one pulse of interest is due to the primary discharge. Both intensity and duration of the pulses are different. This can be related to the different kinetics of elementary processes in the plasma structures. Although these results are obtained by measuring the total light emission from the plasma in the observation region, they represent valuable data of the plasma dynamics of IEC fusion reactor.

Scintillation detectors were one of the first detectors developed to detect radiation, because these detectors could be used with simple photographic film acting as a light sensor. The light sensor can be a photodiode or photomultiplier, as well as photographic film. The choice of the detector depends on the response time desired, the kind of radiation, and its intensity. Scintillation detectors are of several types, classified according to their state –solid, liquid, or vapor – based on their chemical nature (organic or inorganic). The scintillation mechanism itself is dependent on the crystal lattice structure of the scintillator material. Such detectors have been used for the detection of X-ray and neutron radiation created in IEC devices [10].

The generation of x-ray has been investigated experimentally in the IEC fusion reactor using fast radiation detectors based on type of photomultiplier with high anode characteristics, nanosecond time resolution, shielded against electromagnetic interference in the assembly with fast scintillator. In the development of the detector housings special attention is paid to the screening of the pulsed electromagnetic interference occurring at the time of discharge.

The transmission of materials for X-rays up to 30 keV is readily obtained using the Center for X-Ray Optics (CXRO) web site [11]. Aluminum is the most commonly used material for filters. It has good mechanical properties and provides a wide band-pass while also excluding visible light. Thin sheets of solid material absorb X-rays and the transmission of the sheets depends upon the X-ray energy, the material thickness, and the atomic number Z of the material. The transmission of an Al foil that is 18 m thick is shown as figure 6. The X-rays are absorbed in the Al until the X-ray energy gets above 1keV. At the binding energy of the Al 1s electron, 1.53 keV, referred to as the K edge, the X-rays are again strongly absorbed. The foil begins transmitting X-rays again when the X-ray energy rises above 3keV.

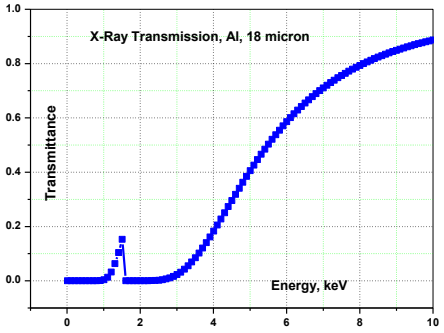

Figure 6. *Graph showing the X-ray transmission of 18m thick sheet of Al, Z=13.*

X-ray yield of hydrogen plasma have been registered by type of photomultiplier shown in figure 7. The temporal distributions of detected x-rays emission are occurring during the initial 1μs.

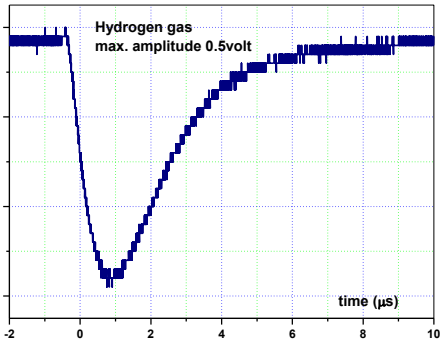

Figure 7. *Temporal evolution of hard X-ray pulse.*

According to the kinetic theory of gases, when gas pressure (or gas temperature) increases, the kinetic energy of gas increases, so it can reach to higher speeds. Therefore, more energetic particles emerge, as a result, more quanta of energy emerges in the form of bremsstrahlung radiations.

When X-rays pass through foils of different material, the intensity of radiation is attenuated according to the relation (Lambert-Beer law), $I = I_0 \exp(-\mu d)$, where I = radiation intensity after passing through matter, I_0 = radiation intensity before passing through matter, d = thickness of the absorber μ = attenuation coefficient (= 1/attenuation length = $1/\lambda$). The attenuation coefficient μ is a function of energy, as the high-energy photons experience less absorption whereas low-energy photons experience high absorption. The attenuation coefficient depends on the X-ray energy and on the absorber material. The attenuation of the incident X-rays as well as effects like heat build-up, scattering and emission of photons with discrete energies are due to interaction of the X-rays with electrons in the atomic shell. The attenuation length ($\lambda = 1/\mu$) of aluminum against the photon energy is shown in Figure 8.

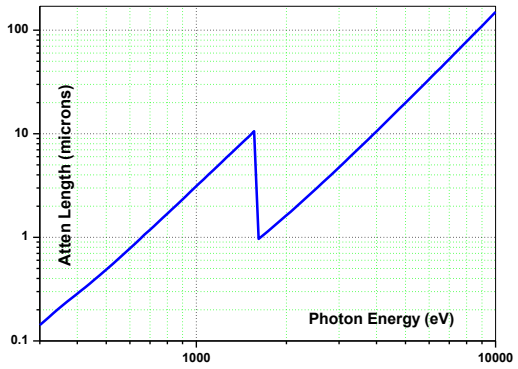

Figure 8. *Attenuation length of photons in aluminum against the photon energy.*

Hydrogen gas is substituted for deuterium or tritium because in this configuration the main function of gas ions is to provide electron Bremsstrahlung emission. Intense emission is concentrated in a small volume surrounding the central axis due to the high electron density formed there. A scintillator photomultiplier tube (SPMT) assembly was employed for the detection of hard X-ray, which was placed at a distance 5 cm away from the evacuated chamber. The scope graph below (Figure 9) is from the experiment ofIEC plasma device when nitrogen is the working gas.

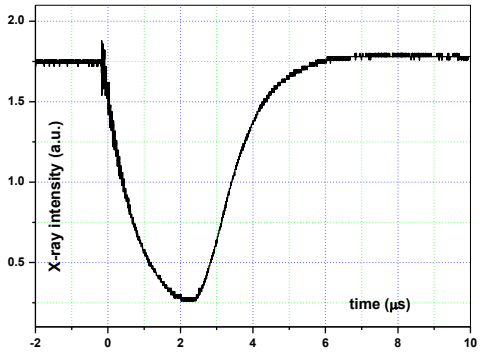

Figure 9. *Signal of scintillation hard X-ray detector for nitrogen plasma.*

Table 2. *Indicates the relative x-ray intensity and FWHM of different gases (nitrogen, hydrogen and helium).*

Gases	Nitrogen	Helium	Hydrogen
Relative X-ray Intensity (a.u.)	0.99	0.697	0.338
FWHM (μs)	2.96	2.73	2.44

Figure 10 indicates that the relation between X-ray intensity and the type of filling gas under operating conditions (P = 0.01 Torr, Vch = 20 kV). It was found that maximum intensity was registered for nitrogen gas when compared with other gases (helium and hydrogen).

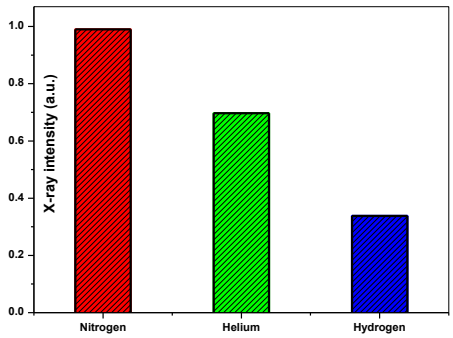

Figure 10. *Relation between x-ray intensity and type of filling gas.*

The measured X-ray intensity is plotted in figure 11 versus the cathode voltage for different pressures. The X-ray intensity increases with an increase of the cathode voltage at constant pressure, and with an increase of IEC chamber pressure at the constant voltage [13].

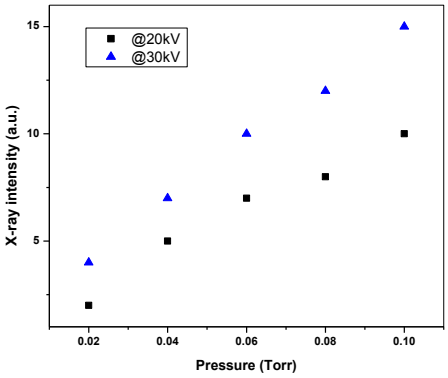

Figure 11. *X-ray production as a function of pressure for different voltages [13].*

The accelerated electrons cause electron-electron collisions in central plasma core region, in other words the energetic electrons scatter in the center of the sphere. The scattering interactions create intense bremsstrahlung x-rays. The emitted x-ray energy is controlled by the grid bias. For mono-energetic electrons, related x-rays occur whenever electrons are rapidly accelerated across a high potential difference. The fraction of the energy in the electron beam that is converted into x-rays (f_x) is given by

$$f_x = 10^{-7} \times Z \times E \tag{1}$$

Where, E is the electron energy in keV and Z is the atomic number of the absorber.

According to relation (1), the anode of the IEC device should be made of Aluminum (lower atomic number) or other light materials for reducing Bremsstrahlung production. The electrons are hitting the anode produces many x-ray photons, these photons reaching the cathode grid. Furthermore, the x-ray photons could release multiple numbers of electrons from the cathode depending on their energy. This phenomenon could be especially significant in pulsed devices due to large currents during a pulse [12].

Temperature was measured by exposing or attaching the thermocouple to the surface to be measured. The multi-meter displays the temperature directly in degrees

Celsius. In this experiment, the thermocouple probe was placed inside of IEC reactor to monitor the gas temperature at 20kV. This thermocouple probe picked up the maximum temperature in its focus as shown in figure 12.

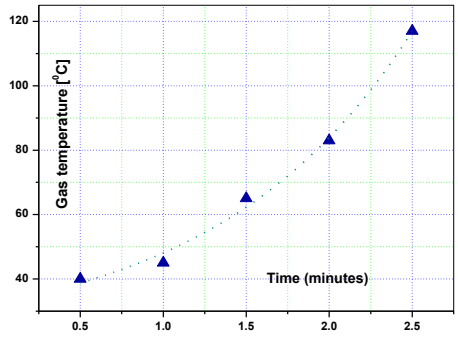

Figure 12. *Gas temperature as function of time.*

4. Conclusions

The IEC fusion device is a powerful source of x-ray radiations which may be suitable for different applications. The same device that produce x-ray yield can be used to generate neutrons yield. The X-ray production threshold depends on E/p of the IEC chamber gas. Furthermore, the electron drift velocity is often expressed as a function of E/p, where E is the electric field and N is the number of molecules per cm^3. Also, the X-ray rate is dependent on the gas choice in the chamber of IEC device. The main mechanism for x-ray radiation should come from interactions of electrons with atoms. Then bremsstrahlung may be the responsible for these emissions. The results encourage the study of other radiations like microwave radio emissions during X-rays measurements using different operating conditions.

Conflicts of Interest

The author declares that there is no conflict of interest regarding the publication of this article.

References

[1] G.H. Miley; S.K. Murali. Inertial Electrostatic Confinement (IEC) Fusion. Fundamentals and Applications; Springer, 2014. ISBN 978-1-4614-9337-2.

[2] Hirsh, R.L. Inertial-Electrostatic Confinement of Ionized Fusion Gases. *J. Appl. Phys.* 1967, 38, 4522.

[3] Hirsh, R.L. Experimental Studies of a Deep, Negative, Electrostatic Potential Well in Spherical Geometry. *Phys. Fluids.* 1968, 11, 2486.

[4] Miley, G.H., et al. Inertial-Electrostatic Confinement: An Approach to Burning Advanced Fuels. *Fusion Sci. Technol.* 1991, 19, 840-845.

[5] Miley, G.H. et al., in Dense Z-pinches (Proc. 3rd Int. Conf.), AIP, New York, 1994, 675.

[6] Thorson, T.A., et al. Fusion reactivity characterization of a spherically convergent ion focus. *Nucl. Fusion.* 1998, 38(4), 495-507.

[7] K. Masuda; K. Yoshikawa; T. Misawa; K. Yamauchi; Y. Takahashi; S. Shiroya; E. Hotta; M. Ohnishi; H. Osawa. Directional detection of nitrogen and hydrogen in explosive by use of a DD-fusion-driven thermal neutron source. Detection of Liquid Explosives and Flammable Agents in Connection with Terrorism, Springer, the Netherlands, 2008, 155-166. ISBN 978-1-4020-8465-2.

[8] Available online: http://www.sodern.com/sites/en/ref/Neutron-Tube_78.html (accessed on 14 December 2017).

[9] McGuire T.J.; Sedwick R.J. Improved confinement in inertial electrostatic confinement for fusion space power reactors. *Journal of Propulsion and Power*, 2005, 21(4), 697-706.

[10] Weidner J.W.; Kulcinski G.L.; Santarius J.F.; Ashley R.P.; Piefer G.; Cipiti B.; Radel R.; Krupakar Murali S. Production of 13N via inertial electrostatic confinement fusion. *Fusion Sci Technol.* 2003, 44(2), 539-543.

[11] Available online: http://www.cxro.lbl.gov/ (accessed on 14 December 2017).

[12] Nadler J.H.; Miley G.H.; Momota H.; Shaban Y.; Nam Y.; Coventry M. Neutron production and ionization efficiency in a gridded IEC device at high currents. *Fusion Technol.* 2001, 39(2), 492-497.

[13] Gamal M. El-Aragi. Building Inertial Electrostatic Confinement Fusion Device Aimed for a Small Neutron Source. *International Journal of High Energy Physics*, 2017, 4(6), 88-92.

[14] H. Ohgaki; I. Daito; H. Zen; T. Kii; K. Masuda; T. Misawa; R. Hajima; T. Hayakawa; T. Shizuma; M. Kando; S. Fujimoto. Nondestructive Inspection System for Special Nuclear Material Using Inertial Electrostatic Confinement Fusion Neutrons and Laser Compton Scattering Gamma-rays. *IEEE Transactions on Nuclear Science*, 2017, 64(7), 1635-1640.

[15] Michael Winter; Helmut Koch. Inertial Electrostatic Confinement Plasma Devices –Potential thruster technology for very accurate attitude control systems. The 35th International Electric Propulsion Conference, Georgia Institute of Technology, USA, 2017, October 8-12.